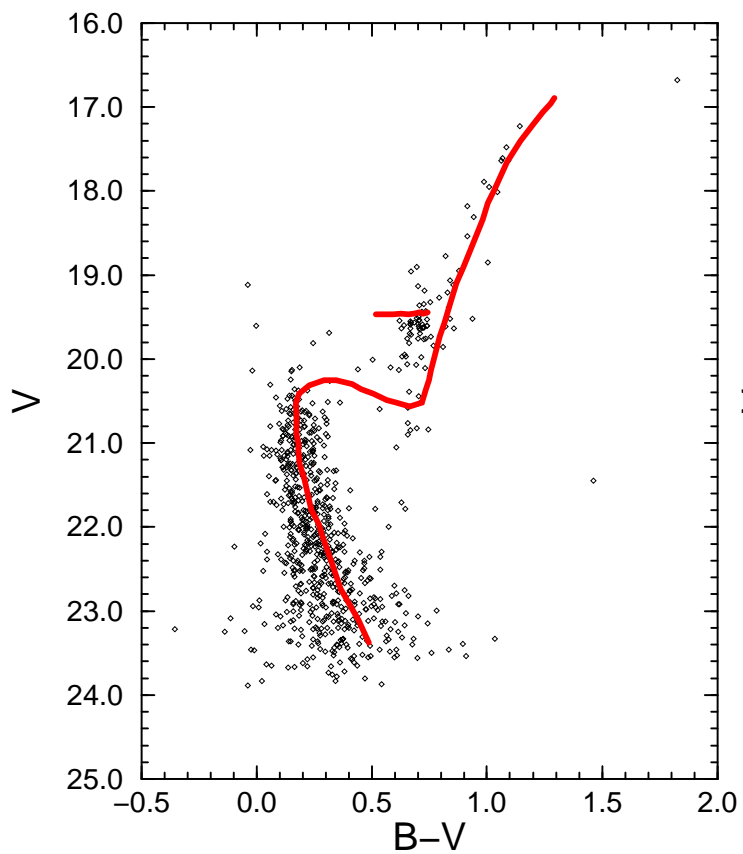
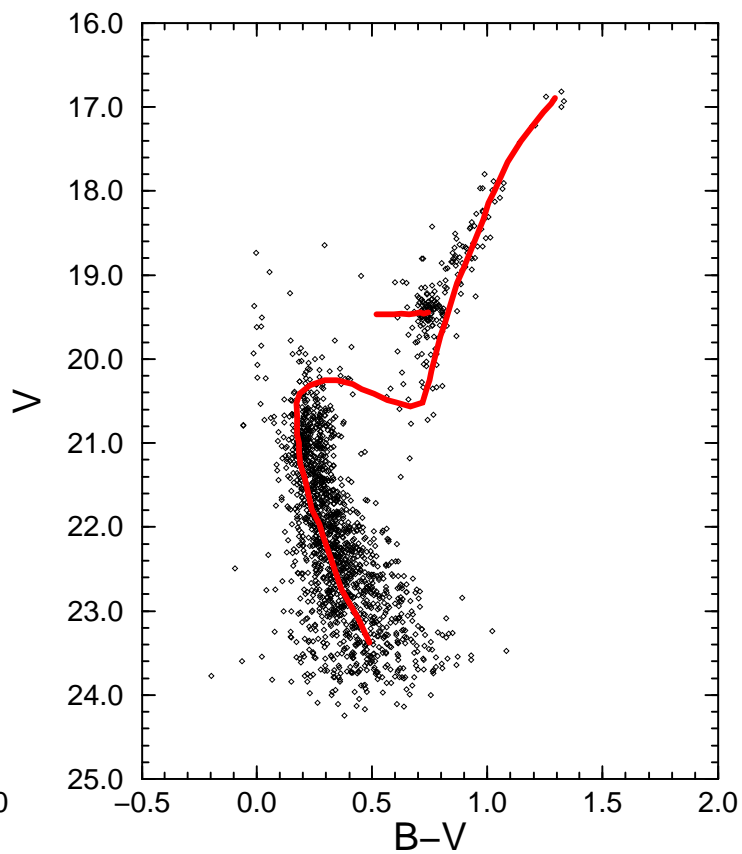


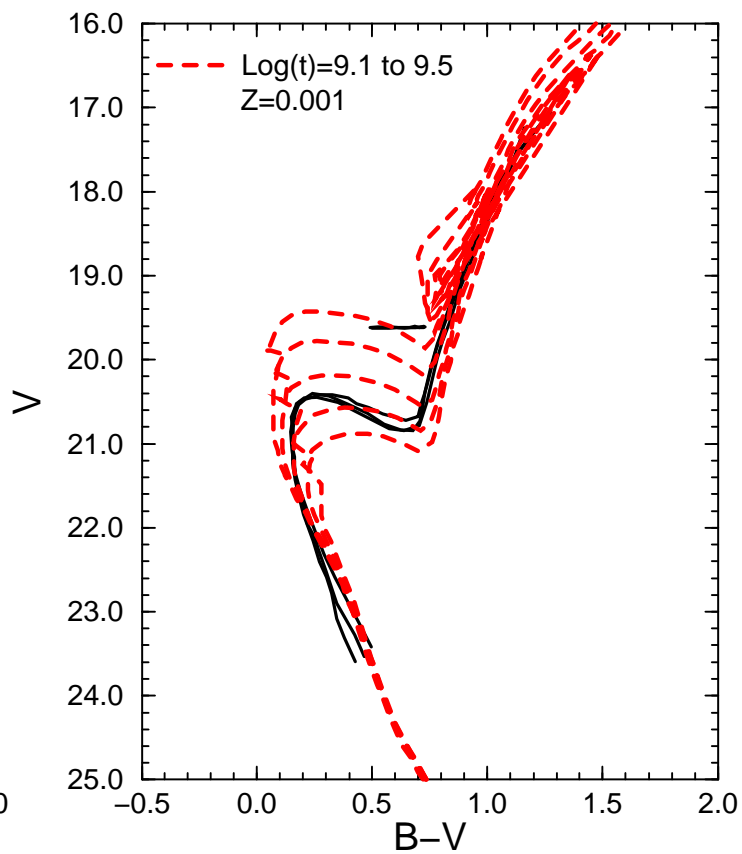
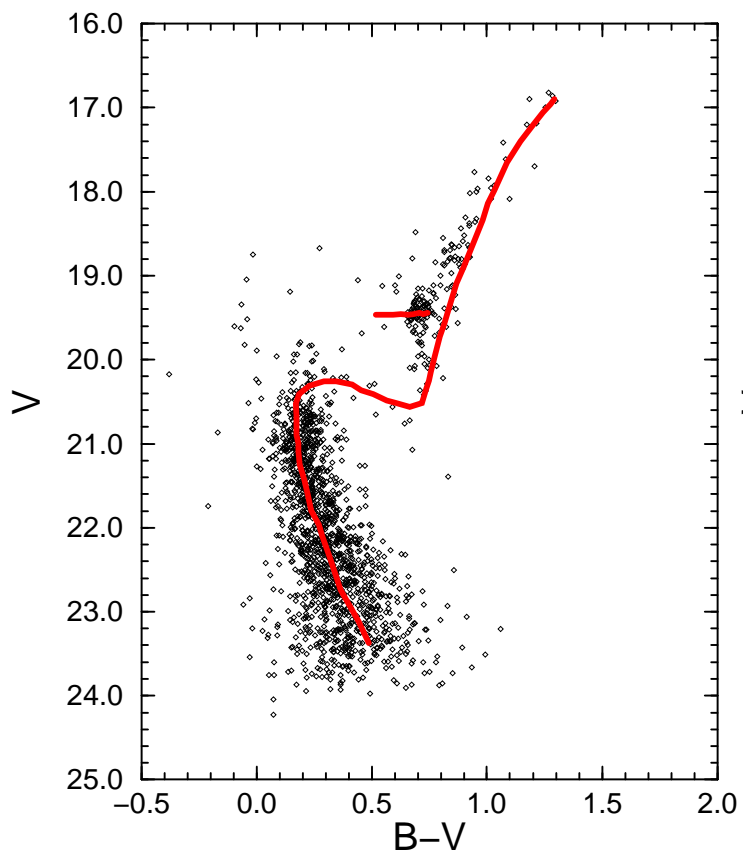
NGC 152



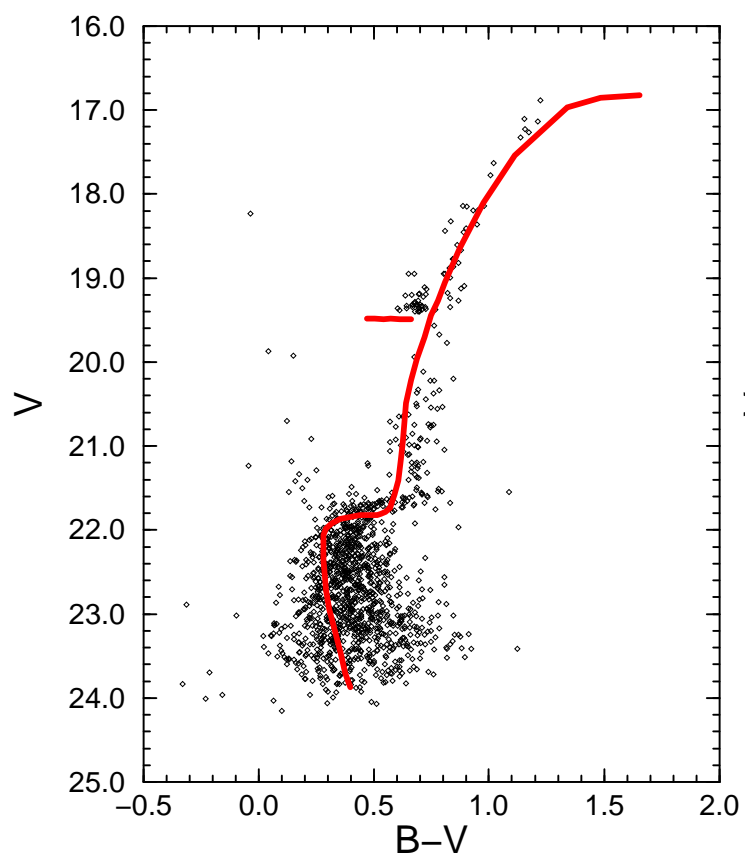
NGC 411



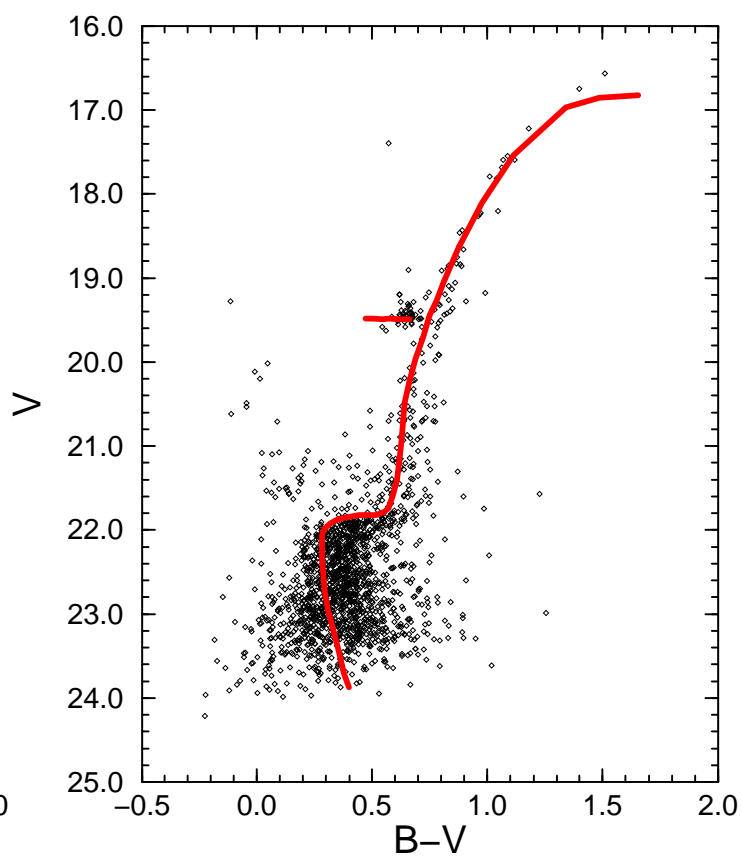
NGC 419



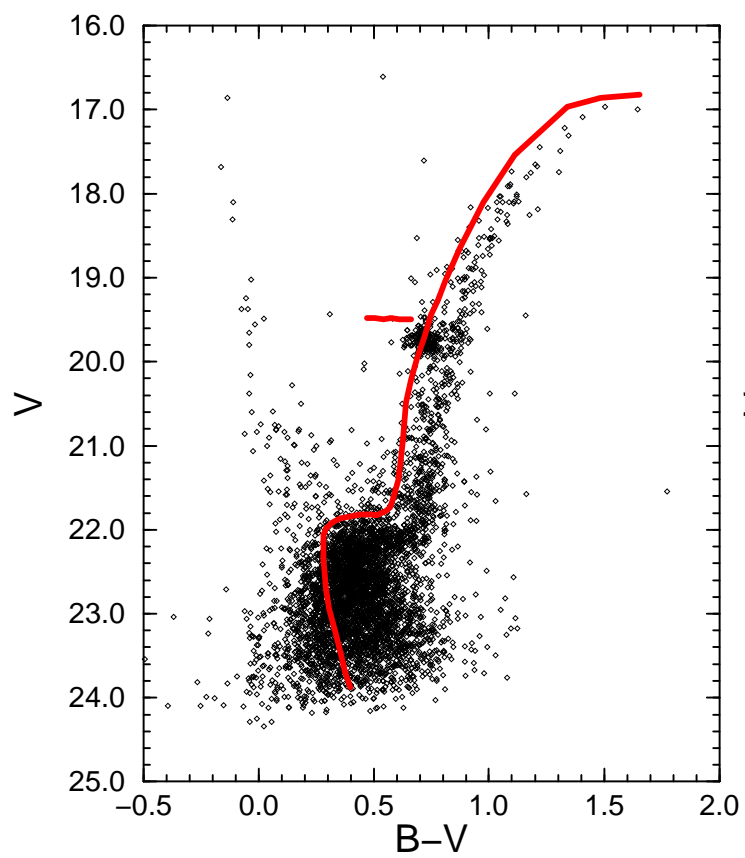
NGC 339



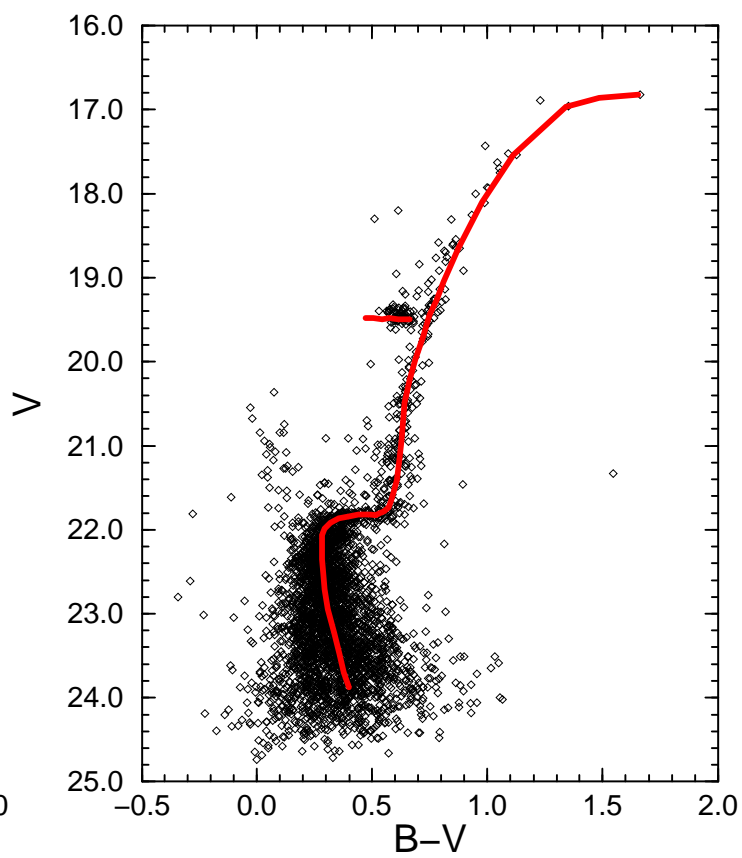
NGC 361

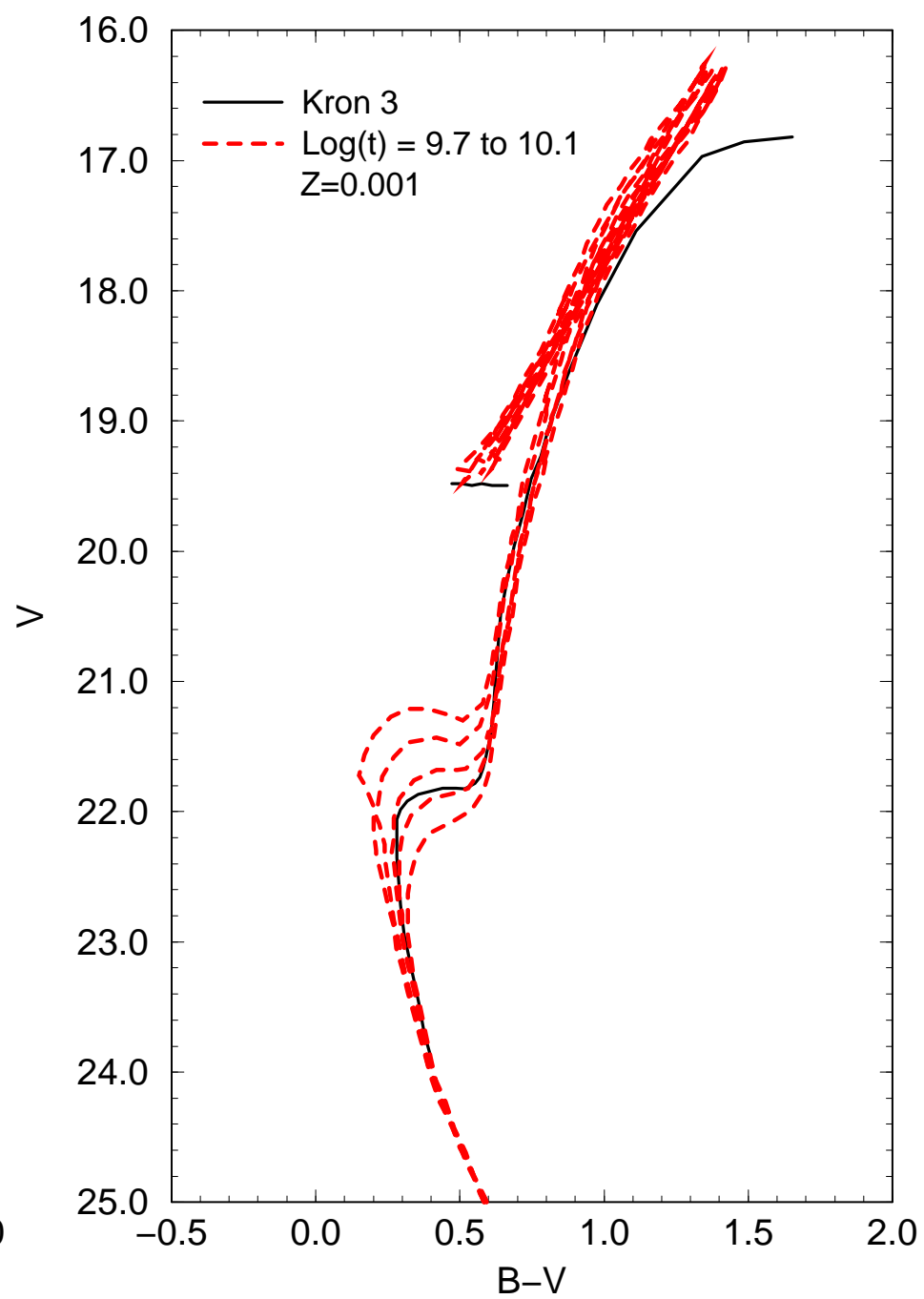
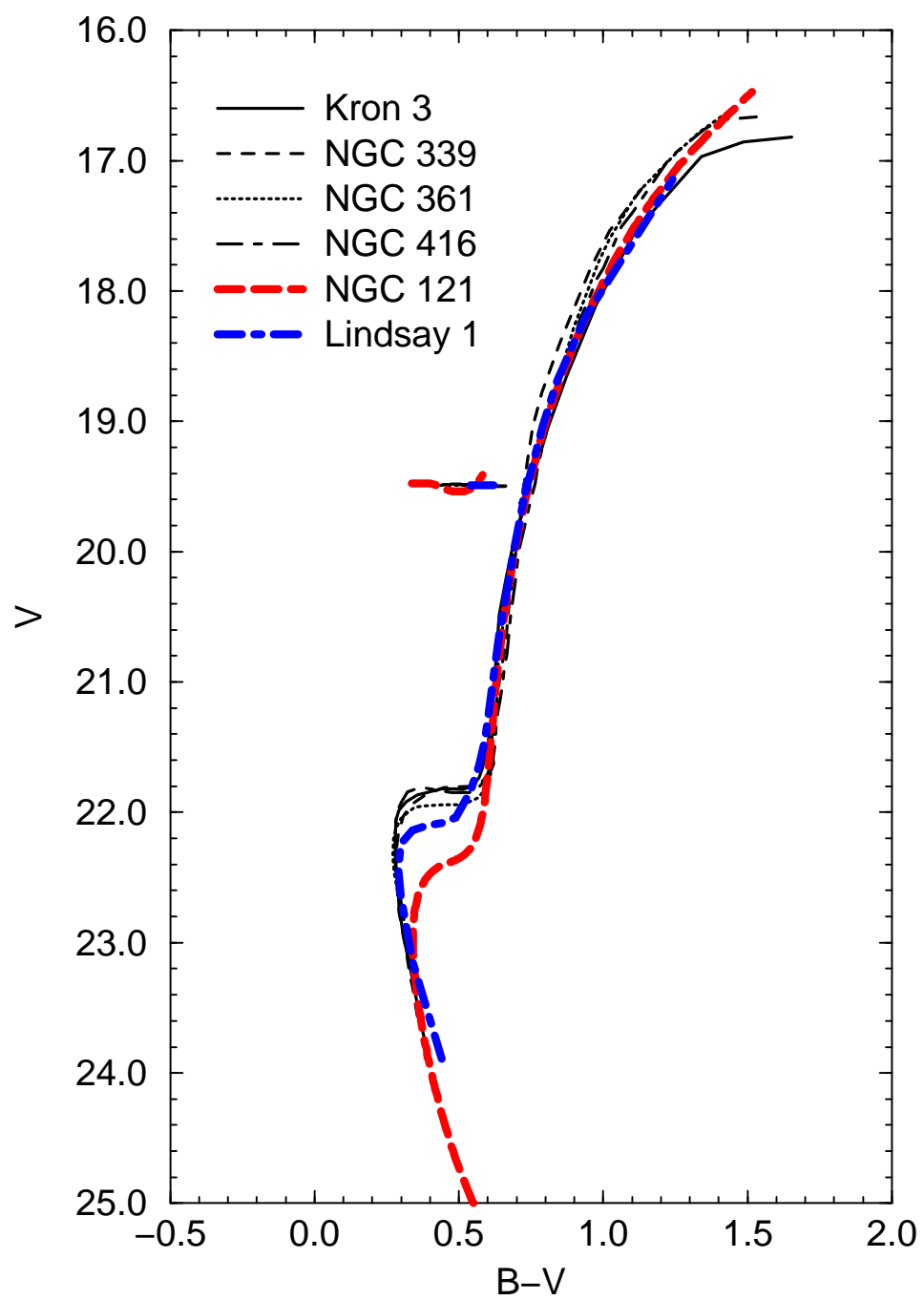


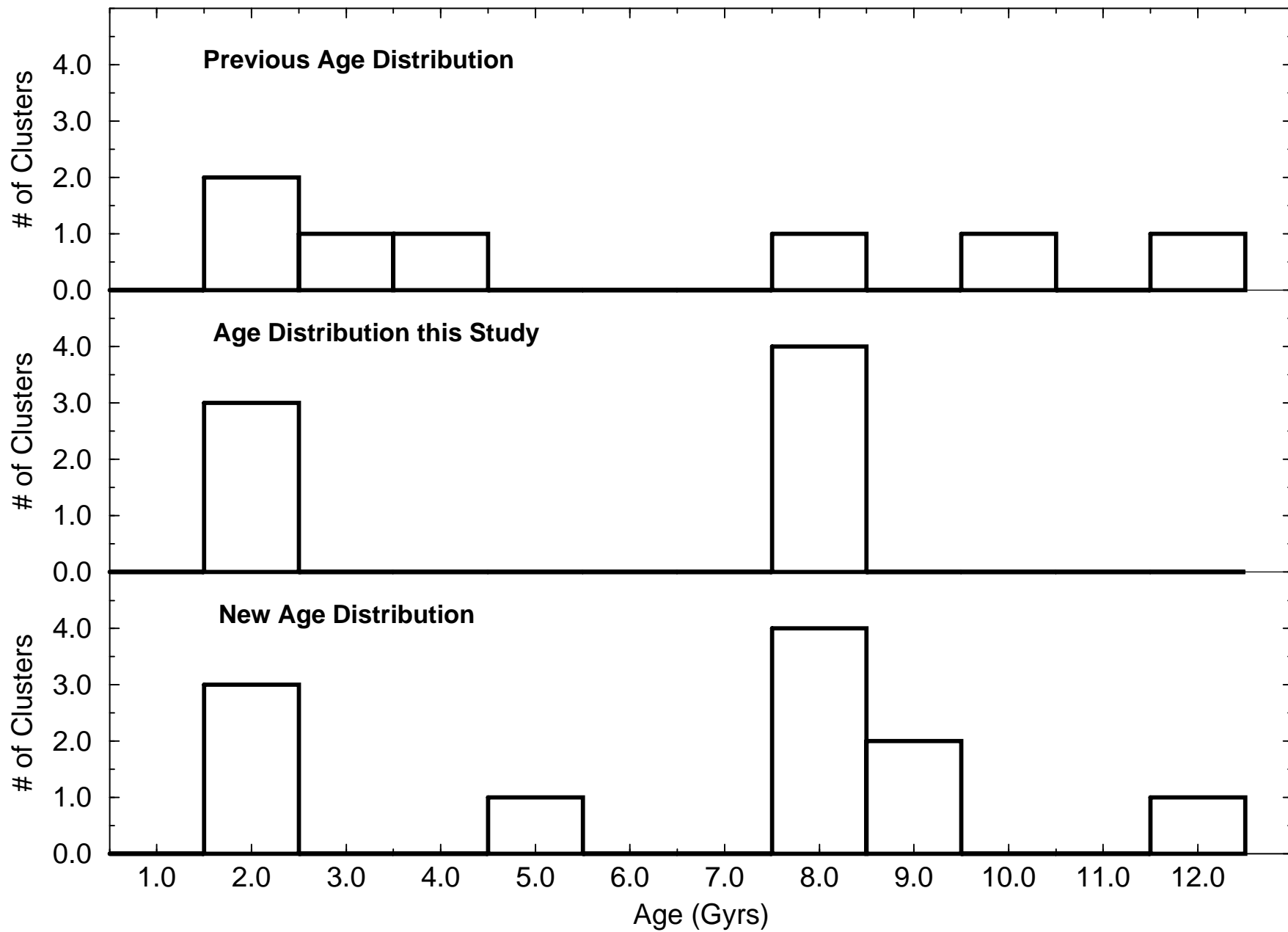
NGC 416



Kron 3







Two Groups of Nearly Coeval Star Clusters in the Small Magellanic Cloud¹

R. Michael Rich

Department of Physics and Astronomy, University of California at Los Angeles
8979 Math-Sciences Bldg, Los Angeles, CA 90095-1562 rmr@astro.ucla.edu

Michael Shara

Space Telescope Science Institute
3700 San Martin Drive, Baltimore MD, 21218 shara@stsci.edu

S. Michael Fall

Space Telescope Science Institute
3700 San Martin Drive, Baltimore MD, 21218 fall@stsci.edu

and

David Zurek

Space Telescope Science Institute
3700 San Martin Drive, Baltimore MD, 21218 zurek@stsci.edu

Received _____; accepted _____

¹ Based on observations with the NASA/ESA Hubble Space Telescope, obtained at the Space Telescope Science Institute, which is operated by the Association of Universities for Research in Astronomy, Inc., under NASA contract No. NAS5-2655.

ABSTRACT

We report new photometry of populous intermediate-age clusters in the SMC using the *Hubble Space Telescope*. In contrast to the accepted picture, these clusters appear to have formed in two brief intervals, one 8 ± 2 Gyr ago, and a more recent burst 2 ± 0.5 Gyr ago. When the ridgelines of the four clusters (NGC 339, 361, 416, and Kron 3) in the 8 Gyr burst are aligned, the dispersion in turnoff luminosities is < 0.2 mag, corresponding to a maximum age spread of ± 0.7 Gyr. When the ridgelines of three clusters (NGC 152, 411, and 419) in the 2 Gyr burst are aligned, the maximum dispersion of 0.2 mag in turnoff luminosity corresponds to a permitted age spread of ± 0.2 Gyr. Within each group of clusters, the entire cluster loci (including red giant branches and clumps) are nearly identical, consistent with indistinguishable metallicities and ages. In contrast to the wide dispersion in ages previously reported in the literature, our sample with more precise photometry and age measurements supports a burst-punctuated rather than a continuous cluster formation history for the 2 Gyr and 8 Gyr SMC clusters.

Subject headings: galaxies: star clusters – Magellanic Clouds – galaxies: evolution – color-magnitude diagrams

1. Introduction

The age distribution of star clusters in the Large Magellanic Cloud (LMC) has long been known to be approximately bimodal (van den Bergh 1991; vdB91, Westerlund 1997), while the Small Magellanic Cloud (SMC) is considered to have formed its clusters continuously over the last 12 Gyr (Olszewski, Suntzeff, Mateo (1993; OSM93, vdB91). The ages of the Magellanic clusters have been difficult to measure because of stellar crowding, field star contamination, and faintness of the main sequence turnoffs. The availability of large aperture telescopes and electronic detectors have vastly increased the number of Magellanic clusters with age determinations. In the age range from 1-14 Gyr, where the cluster ages potentially preserve the fossil record of ancient cluster formation and disruption history, the LMC has a period from 2.5-12 Gyr in which only one star cluster (ESO121-SC03) appears to have been formed (OSM93). In contrast, existing data suggest that the SMC was more or less continuously forming clusters during this interval (Mighell et al. 1998). Furthermore, the oldest clusters in the LMC appear to be approximately as old as the oldest globular clusters in the Galaxy (Mighell et al. 1996, Olsen et al. 1998, Johnson et al. 1999) while the oldest cluster in the SMC is distinctly younger (Stryker et al. 1985, Shara et al. 1998). It has been argued (vdB91) that the disparate timing of these bursts is inconsistent with scenarios in which cluster formation was triggered by encounters between the SMC and LMC.

Much of our understanding of the evolution of the Magellanic Cloud/Galaxy system is limited by the depth and accuracy of ground-based photometry. Further, the derived cluster ages are not consistent, both due to the use of different telescopes, filters, and detectors, and due to the different isochrones used to fit the main sequence turnoff. Finally, ground-based color-magnitude diagrams must avoid the cluster cores because of crowding and thus suffer serious contamination by field stars.

In order to obtain a large, uniform sample of Magellanic Cloud cluster photometry, we have undertaken a survey of short-exposure images in the cluster cores using the HST. The results on nearly 50 clusters will be described elsewhere (Rich et al. 1999). Taking advantage of this uniquely homogeneous and high quality data set, we focus here on our sample of 7 SMC clusters with ages > 1 Gyr, in which we find evidence for two remarkable bursts. Our sample of SMC clusters includes all clusters with $V < 13$ and $(B - V) > 0.5$ in Table II of van den Bergh’s (1981) compilation. We therefore determine ages for the most luminous ($M_V < -6$) old SMC clusters – those which most closely resemble their Milky Way counterparts.

After producing the color-magnitude diagrams we noticed that our sample naturally divides into two groups of clusters within which there is very little dispersion in age or metallicity. The following section describes our photometry and method for comparing the cluster color-magnitude loci. Section 3 describes our age determination for the 2 and 8 Gyr cluster groups using the most straightforward method of measurement, the magnitude difference between the horizontal branch and the turnoff point and the equivalent approach using isochrone fitting. In this section, we also consider the minimum possible age dispersion among these clusters. Section 4 considers the maximum age dispersion that could be derived from our data. We consider our new finding relative to what is already known about the oldest SMC clusters in Section 5, and we report our conclusions in Section 6.

2. Photometry and Color-magnitude Diagrams

The SMC clusters were observed as part of a snapshot survey using WFPC2 on board the *Hubble Space Telescope*. Table 1 gives the log of observations; all exposures were shorter than 600 sec, and were obtained through the F450W and F555W filters (one frame per color). The frames were reduced according to the HST pipeline; however we have used

the best calibrations available rather than accept the data as processed near the time of acquisition.

Magnitudes were measured from the images using the point-spread function (PSF) fitting program ALLSTAR in the DAOPHOT II environment (Stetson 1994a,b). The PSF's were created for each cluster in each color by using the standard approach of subtracting neighboring stars from every star contributing to the PSF, a procedure that is repeated until it is judged that there is no improvement between iterations. For the first cut aperture photometry, we use a 3 pixel aperture. The final photometry must be corrected to a large aperture of 0.5" (or 11 pixels on the PC). The aperture correction is measured for PSF stars from which the near neighbors have been subtracted. This produces an aperture correction for each image (Table 2) which varies due to small changes in the HST focus. Because most of the observations were taken before the cool down of the WFPC2 on 23 April 1994, a correction (Table 3) for the throughput difference is made (HST Data Handbook: WFPC2 Photometric Corrections). To be complete, we have also included a small correction for the contamination that accumulates between warm-ups of the cameras; this is a very small effect for optical magnitudes (Table 4). Finally, the photometry was transformed to B and V respectively as described in Holtzman et al. 1995b.

2.1. Color-Magnitude Diagrams

The color-magnitude diagrams resulting from the photometry naturally divide into two groups based on the magnitude difference between the red horizontal branch and the main sequence turnoff point. For NGC 411, 152, and 419 this difference is about one magnitude, while it is about 2.5 magnitudes for Kron 3, NGC 339, 361, and 416. We overplot the ridgeline of NGC 411 in the younger group (which we name the NGC 411 group) and we overplot that of Kron 3 relative to the older "Kron 3" group of clusters.

Within each group of clusters, it is clear that the color-magnitude arrays are remarkably similar. It is especially noteworthy that the age-sensitive turnoff to horizontal branch magnitude difference, and the metallicity sensitive giant branch position, is very similar with each group. While the similarity is evident in the Kron 3 group, the ridgeline does not overplot those data perfectly. However, if the Kron 3 ridgeline is shifted by eye, the agreement with each of the other older clusters is excellent; we thus speculate that the dispersion in the apparent clump luminosity could be due to a dispersion in distance, extinction, or calibration uncertainty. To study further the possible similarity of clusters within each group, we fit empirical ridgelines by eye to each cluster and shift them freely to coincide with the NGC 411 ridgeline (younger group) and Kron 3 ridgeline (older group) respectively. The dispersion in relative ages and metallicities can be compared within each group, even though the distance modulus to any individual cluster is relatively uncertain.

The empirical cluster ridgelines are the result of a freehand fit by eye to the color-magnitude diagrams. The ridgelines are given in Tables 6-8. Within each group, these CMD loci are nearly identical. We have exploited these similarities and shifted the loci in V and $B - V$ to match Kron 3 in the case of the older clusters, and NGC 411 for the younger clusters. We report the shifts required for the clusters to coincide with the designated templates in Table 9, which also gives the mean luminosity of the red clump for these clusters. Given the many corrections required to our data to establish the calibration, we consider our zero points to be accurate to ≈ 0.05 mag.

It is interesting to note the small dispersion in red clump luminosities for the clusters. The old clusters have $V = 19.46 \pm 0.19$ and the young clusters have $V = 19.50 \pm 0.08$, neither being statistically different from the sample mean of $V = 19.48 \pm 0.14$. We find no evidence that the luminosity of the red clump differs between these groups of clusters, which would be expected from theoretical calculations that find little dependence of clump

luminosity on age or metallicity (cf. Sweigart, Greggio & Renzini, 1990; Castellani, Chieffi & Straniero 1992; Girardi et al. in preparation). The red clumps of our clusters are fainter than the clump for the SMC field of $V = 19.25 \pm 0.05$ derived from the data of Udalski et al. (1998). We note, however, that the mean V was calculated by adding an approximate $V - I$ for the clump to the derived peak I magnitudes of Udalski et al.

3. Cluster Age Measurements

The apparent shifts among the clusters in the Kron 3 group are due either to differing distance modulus, reddening, or calibration uncertainties. However, we focus our efforts on learning as much as possible from the similarity of the color-magnitude arrays and loci within each group. The best constraint on relative ages is the ΔV_{TO}^{HB} index, the magnitude difference between the turnoff and the horizontal branch. The main sequence turnoff luminosity fades with increasing age, while the HB luminosity is determined by the mass of the helium burning core, which is roughly constant in low-mass stars. The age is derived by using various calibrations of ΔV_{TO}^{HB} versus age and metallicity from the literature (e.g. Walker, 1992). The age may also be derived by fitting the isochrones to the red clump rather than shifting the isochrones by a prescribed distance modulus and reddening. Although this method relies on essentially the same fundamental physics, the isochrones are fit to the entire color magnitude diagram and the result is less sensitive to the increase of errors at faint magnitudes. In our first approach to exploring the age dispersion of the clusters, we shift the ridgelines to agree as closely as possible with the template cluster and then determine the maximum age dispersion among the clusters implied by this procedure. In Section 4, we will also consider the age dispersion derived from independent fits to the apparent color-magnitude arrays of each cluster.

3.1. The 2 Gyr Old Burst

We consider three intermediate-age clusters, which we designate the NGC 411 group. Figure 1 illustrates the unshifted NGC 411 ridgeline overplotted on the data of NGC 411, 152, and 419. The cluster loci are identical to within observational uncertainty, after the offsets in Table 9 are applied. A fit to the red clump using the $Z=0.001$ Bertelli et al. (1994) isochrones (consistent with $[\text{Fe}/\text{H}]=-0.9$ from Da Costa & Mould 1986) gives 2.0 ± 0.2 Gyr. Because the fit of the red giant branch is good, we conclude that the metallicity of the isochrones is in good agreement with the data. In order to explore the possible spread in age within the 2 Gyr group, we must know the maximum possible spread in metallicity between these clusters. We estimate the permitted dispersion in metallicity from the rate of color change in the red giant branch locus as a function of metallicity, as measured from the isochrones from the isochrones. Just below the RGB tip, this is approximately $\Delta[\text{Fe}/\text{H}] = 3.1\Delta(B - V)_0$ and the entire spread in the 2 Gyr clusters corresponds to 0.15 dex in metallicity. The nearly perfect agreement of the full cluster ridgelines (including the red giant branches) within this group of clusters is remarkable, and admits very little variation in age, metallicity, or any other significant parameter.

The age estimate from ΔV_{TO}^{HB} (Walker 1992) gives $1.65 < t_{Gyr} < 2.05$. The lowest age would apply for $\Delta V_{TO}^{HB} = 1.1$ mag and $[\text{Fe}/\text{H}]=-1.1$, while the largest age would correspond to $\Delta V_{TO}^{HB} = 1.3$ and $[\text{Fe}/\text{H}]=-1.6$. In fact, the range due to the difficulty of locating the nearly vertical turnoff point in the noisy data rather than an actual dispersion, and the metallicity differences within this group are also almost certainly smaller than stated. Our preferred estimate from this method is an age of 1.85 ± 0.1 Gyr for the NGC 411 group.

The turnoff point of a young star cluster will fade more rapidly with age than that of an older cluster, such as those in the Kron 3 group discussed below. Buonanno et al. 1993 give $\Delta \log t_9 = (0.44 + 0.04[Fe/H]\Delta M_V(TO))$, and the small dispersion in relative cluster

loci constrains the full age spread to be less than 0.4 Gyr. If all of the cluster ridgelines are forced to coincide and the isochrones are superposed, then direct inspection of the result (Figure 1) suggests that the full age dispersion could be as small as 0.2 Gyr, or 10% of the age of the clusters.

3.2. The 8 Gyr Old Burst

In Figure 2, we display the color-magnitude diagrams of the four SMC clusters in the older of the two bursts, which we designate the “Kron 3” group. We have overplotted the empirical Kron 3 ridgeline on all four CMDs, without applying any magnitude or color shifts. The nearly precise agreement of the Kron 3 ridgeline with the ridgelines of NGC 339, 361, and 416 is striking. The combination of nearly identical main sequence turnoffs, red giant branches, and clumps is consistent with a very small dispersion in age or metallicity within this group of clusters. In contrast to the other clusters in this group, NGC 416 is superposed near the center of the SMC, and we speculate that it may well be reddened relative to the other clusters (explaining its fainter and redder clump and locus). We will return to the reddening of the clusters in Section 4. Although WFPC2 photometry of the oldest SMC clusters has been reported in the literature before (Mighell et al. 1998) our photometry of these clusters is permits us to see clearly delineated the turnoff point, subgiant branch and 1-2 mag of main sequence.

Figure 2 also shows our best fit (isochrones force-fit at the red clump) using the $Z=0.001$ (corresponding to $[Fe/H]=-1.27$) Bertelli et al. (1994) isochrones, which yields an age of 8.0 ± 0.5 Gyr. Recent Ca index abundance measurements by Da Costa & Hatzidimitriou (1998) give -1.12 dex for Kron 3 and -1.46 for NGC 339; our isochrones are consistent with this range of metallicity. Applying the age-sensitive magnitude difference between the turnoff and HB, ΔV_{TO}^{HB} , we find $\Delta V_{TO}^{HB} = 2.85 \pm 0.1$ mag. However, the large

errors below the turnoff make it difficult to clearly locate the V magnitude of the bluest excursion of the isochrone which defines the turnoff point. However, if the red clumps of these clusters are forced to coincide, the full dispersion in the V magnitudes of the flat subgiant branches (a much better defined point on the color-magnitude diagrams) is 0.2 mag. This is in good agreement with the dispersion in ΔV_{TO}^{HB} . Were we to use the extreme assumption that the youngest cluster has $[\text{Fe}/\text{H}]=-1$ while the oldest has $[\text{Fe}/\text{H}]=-1.66$ we would find the maximum permitted age spread to be 7.5 ± 0.3 Gyr. If the metallicities of the clusters are nearly identical this spread reduces to ± 0.1 Gyr.

If the cluster ridgelines are force-fit to the best coincidence possible, the maximum dispersion at the turnoff is 0.1 V mag. Using the formula of Buonanno et al. (1993) referred to in Section 3.0, we find that the maximum 0.1 V mag dispersion around the age of Kron 3 corresponds to ± 0.04 dex in age. For a mean age of 8 Gyr the total duration of the burst is ± 0.7 Gyr, or a full range of 1.4 Gyr. Inspection of the Bertelli et al. (1994) isochrones (Figure 2) suggests that the entire age spread is likely smaller than this, of order 1 Gyr.

4. Are the Bursts Real?

Our evidence for two bursts is based on the extraordinary agreement of the cluster loci when forced to coincide. This similarity reduces to agreement in the ΔV_{TO}^{HB} index (age) and in the red giant branch locus (metallicity). Ages are usually determined by shifting isochrones according to distance and reddening and comparing the data to the turnoff in the isochrones. This approach works poorly when distance and reddening is imprecisely known as is the case with the SMC clusters. In order to test more rigorously the narrowness of these bursts, we take 3 approaches toward age determination, all of which derive from fitting the Bertelli et al. (1994) isochrones under different assumptions: (1) We tie the horizontal branch of the isochrones to the cluster red HB. This is the equivalent of using

the ΔV_{TO}^{HB} method of age determination. (2) We have shifted the isochrones according to the SMC distance modulus plus total absorption based on the reddening derived for each cluster from the shifts in Table 6. This method assumes that the color shifts are due to reddening. (3) We derive ages by placing the isochrones using the vdB91 values for the distance modulus (18.93 mag) and reddening (0.04 mag). Method (3) assumes that the color shifts are perhaps due to an internal calibration error rather than measuring actual differences in reddening.

Table 10 gives the summary of ages derived for the clusters using the 3 methods, and Table 11 gives the age range for the young and old clusters, for $[\text{Fe}/\text{H}] = -1.71, -1.31$, and -0.71 . For the young clusters, the best fits for the isochrones were between the two high metallicities, while the best fits for the old clusters occurred at the metal poor end, qualitatively in agreement with Da Costa & Hatzidimitriou (1998). For the 2 Gyr burst clusters, the full range of ages measured from fits of the isochrones is $1.0 < t_{\text{Gyr}} < 2.11$, however the smallest range was 1.6-2.1 Gyr, using the HB fitting method. Even allowing for a full variation in metallicity and age determination method, we find that the 3 young clusters formed within a span of 0.5 Gyr in a burst approximately 1.5 Gyr ago.

For the Kron 3 clusters, the full permitted age range of isochrone fits, varying all the parameters, is 5-10 Gyr. However, as Table 10 shows, the age range in each entry is never larger than 2.6 Gyr and usually much smaller. It is striking that when the HB fitting method is employed, the full range in permitted ages is $7.9 < t_{\text{Gyr}} < 8.9$ spanning the range -1.71 to -1.31 dex. The other two methods assume identical distance and reddening for all the old clusters; as mentioned earlier, these assumptions lead to an age range that is inconsistent with the excellent agreement in ΔV_{TO}^{HB} between the different CMDs. The outlier NGC 339 has a brighter clump than the other clusters and may well lie 0.1 mag closer than the SMC while NGC 416 is almost certainly reddened. We conclude that the 8

Gyr old burst is also real.

It is instructive to consider in detail the implications of trying to determine the ages and dispersion in ages using the standard method of correcting the isochrones for the distance modulus and reddening. If we assume that the Kron 3 group lies at the SMC distance modulus and that the shifts are due to reddening alone, the implied dispersion in age is large. The greatest contribution to a possible formal age range would be a spread in metallicity: NGC 339 could be as young as 3.1 Gyr with $[\text{Fe}/\text{H}]=-0.71$, and Kron 3 could be as old as 8.3 Gyr if its $[\text{Fe}/\text{H}]=-1.71$, a range of 5.3 Gyr. However, the lowest metallicity isochrones actually fit best while the more metal rich isochrones are redder than the data. Fitting with isochrones of the same (lowest) metallicity, the age range permitted would be 2.6 Gyr. We note that NGC 339 has the brightest observed red clump of the entire sample, at $V = 19.28$; at any metallicity its age is found to be 1.5 Gyr younger than the other clusters in the Kron 3 group. We prefer the hypothesis that NGC 339 is ≈ 0.1 mag closer than the bulk of the SMC. If we were to assume that all the clusters lie at the distance of the SMC then the derived age range 3-5 Gyr implies a 0.6-1.1 mag spread in ΔV_{TO}^{HB} using the formula of Walker (1992) which would be clearly in disagreement with the data.

In our opinion, the best measurement of relative ages for this data set is the use of the ΔV_{TO}^{HB} method or the equivalent method of fitting the Bertelli isochrones at the red clump. These approaches might be considered to be the “minimum age spread” solutions. However, the assumption of little age spread produces no additional observational complications other than requiring that some combination of distance and reddening produce a 10 – 20% dispersion in the apparent moduli of the clusters. Nor surprisingly, both of our methods based on the red clump yield a dispersion in age of 10% within each burst.

On the other hand, if we assume that all the clusters are at the same distance and reddening and blindly fit the isochrones (or alternatively, take our measured color-shifts as

being due to reddening alone) we find much larger age dispersions. The full range in age required would in turn demand a large dispersion in ΔV_{TO}^{HB} that we do not observe, and that would not be consistent with the isochrones themselves.

4.1. Implied Dispersions in Distance Modulus and Reddening

We have shown that the ridgelines of clusters in the NGC 411 group are nearly identical. Further, there is also little dispersion in the reddening and distance moduli of the clusters in this group. On the other hand, the Kron 3 clusters have similar ridgelines, but have a 0.4 mag dispersion in the apparent brightness of the red clump (see Figure 2). The discrepancy is especially evident for NGC 416. The total dispersion in V magnitude for the Kron 3 clusters implied by both the shift method and the apparent V magnitude of the red clump is ≈ 0.4 mag. The two most discrepant clusters are NGC 416 and NGC 339. These clusters have loci 0.1 mag redder than Kron 3, and if due to reddening in the direction of these clusters, we must deredden both NGC 416 and NGC 339 and their 0.4 mag difference remains. If dereddened by 0.31 mag in V and 0.1 mag in $B - V$, the clump luminosity and locus of NGC 416 would be nearly identical to that of Kron 3. Dereddening NGC 339 as required by its shift forces its red clump 0.43 mag brighter than Kron 3. At a modulus of 19.0, the total magnitude dispersion would correspond to a depth along the line of sight of $\approx 20\%$ or ≈ 10 kpc ($\approx 10^\circ$ on the sky), if all of the dispersion were due to the depth of the pop II halo of the SMC (Westerlund 1997). Because in fact NGC 339 accounts for nearly all of this dispersion, we do not take this as an estimate of the depth of the SMC halo.

5. The Oldest Clusters

How do the clusters in the Kron 3 group compare with the oldest known SMC clusters? Figure 3 compares the ridgeline of Kron 3 with those of NGC 121 and Lindsay 1 (Olszewski, Schommer, & Aaronson 1987). NGC 121 remains the oldest SMC cluster, followed by Lindsay 1 (2 Gyr younger) and our Kron 3 group of clusters (4 Gyr younger than NGC 121). Although the data sets for the old clusters include ground-based photometry, we have redetermined the ages of these clusters using our isochrones, in order to have a consistent set of age measurements. The 8 Gyr age determined above for the Kron 3 clusters is consistent with the 12 Gyr age of NGC 121 (Stryker et al. 1985; Shara et al. 1998). We derive an age of 10 Gyr for Lindsay 1, in good agreement with Olszewski et al. (1987). While we find evidence that the Kron 3 group is coeval, the old clusters NGC 121 and Lindsay 1 clearly differ in age from each other and from this group; the oldest SMC clusters were not formed in a single short burst event.

6. The Inferred Cluster Formation History

It has long been accepted that the SMC has formed clusters continuously during the past 12 Gyr. Our revised formation history is illustrated in Figure 4. While the absolute age scale may change depending on the choice of age indicator, the strikingly small duration of these bursts is established via the empirical comparison of the new, homogeneous, HST cluster color-magnitude diagrams, which are identical within each group. Referring back to Figure 2 we note the close agreement of the giant branches for all of the old SMC clusters, and we find no measurable dispersion in $[\text{Fe}/\text{H}]$ within the clusters in the age range $8 < t_9 < 12$ Gyr.

Figure illustrates our findings in comparison with the roughly continuous cluster

formation history presented in Westerlund (1997) and other reviews. We also illustrate the burst history for the most luminous ($M_V < -6$) SMC clusters, which include all of those imaged in our HST study. Except for NGC 121, which is clearly older than the 8 Gyr burst, these luminous clusters all formed in either of the 2 or 8 Gyr bursts. In the lowest panel of Figure 4 we include an additional 3 clusters from the literature, all of which have $13 < V < 14$ ($-6 < M_V < -5$): Lindsay 1 (Olszewski, Schommer, & Aaronson 1987), Lindsay 11 (Mould, Jensen, & Da Costa 1992), and Lindsay 113 (Mould, Da Costa, & Crawford 1984). Our ages for these clusters, derived from ΔV_{TO}^{HB} (and using Walker’s 1992 formula), are ≈ 9 Gyr for Lindsay 1 and 113, and ≈ 5 Gyr for Lindsay 11. These ages are larger than those reported by the authors, who fit the Yale isochrones. The age distribution in the lower histogram is 85% complete to $V \approx 14$. Although the sample sizes are too small to draw any significant conclusion, it is interesting that most of the luminous clusters formed in two discrete bursts.

Given the apparent burst history and wide spatial separation of these clusters, we believe that it is premature to consider the notion of an age-metallicity relationship for the SMC clusters. The notion of chemical evolution contains the implied assumption that enriched material from starbursts is incorporated into later generations of stars. Given the widely spaced separation of the clusters and the punctuated nature of the star formation, it is possible that any enrichment of the interstellar medium occurring as a consequence of the formation of these clusters affected field stellar populations of the SMC and not the abundances of later star clusters. Note that the age- metallicity relationship shows almost no change in the abundances of clusters during the interval 5-10 Gyr ago (Da Costa & Hatzidimitriou 1998; Mighell et al. 1998) It will be valuable to obtain detailed abundances for a complete sample of SMC clusters, including the less luminous clusters that we have not considered in this study.

Clusters can be destroyed as well as formed, however we note that it is only the most luminous clusters that display the burst history. We have difficulty imagining a destruction mechanism that would spare the less luminous clusters and leave two neatly concentrated age groupings.

Ground-based color-magnitude diagrams yielded ages that were consistent with a roughly continuous distribution of cluster ages that filled in the period of the LMC gap, the range of 2-14 Gyr. We agree that the SMC formed clusters in that period, but we find evidence that the most luminous clusters were formed in concentrated bursts. As with the case of the field population of the LMC, we find another example where large scale star formation has occurred in bursts. It is also interesting that clusters spaced widely apart have such similar metal abundances and ages. These findings will require more complicated chemical evolution models, and perhaps treating the field and star clusters separately.

If we were able to observe an LMC-like galaxy at half the Hubble time when the Kron 3 group was forming, we might observe four widely separated bursts of star formation. As many high redshift galaxies have such a blotchy appearance, it is interesting to speculate that we observe in these two groups of clusters the fossil record of such events.

Support for this work was provided by NASA through grant number GO-5475 from the Space Telescope Science Institute, which is operated by AURA, Inc., under NASA contract NAS5-2655.

REFERENCES

- Bertelli, G., Bressan, A., Chiosi, C., Fagotto, F., & Nasi, E. 1994, *A&A Supp.* 106, 275
- Buonanno, R., Corsi, C.E., & Fusi Pecci, F. 1989 *A&A*, 216, 280
- Buonanno, R., Corsi, C.E., Fusi Pecci, F., Richer, H.B., & Fahlman, G.G. 1993, *AJ*, 105, 184
- Castellani, V., Chieffi, S. & Straniero, O. 1992, *ApJS*, 78, 517
- Da Costa, G.S. & Mould, J.R. 1986, *ApJ*, 305, 159
- Da Costa, G.S. & Hatzidimitriou, D. 1998 *AJ*, 115, 1934
- Girardi, L., Groenewegen, M.A.T., Weiss, A., & Salaris, M. 1998, *MNRAS*, 301, 149
- Holtzman, J.A. et al. 1995a, *PASP*, 107, 156
- Holtzman, J.A. et al. 1995b, *PASP*, 107, 1065
- Jensen, J., Mould, J., & Reid, N. 1988, *ApJS*, 67, 77
- Johnson, J., Bolte, M., Stetson, P.B., Hesser, J.E., & Somerville, R.S. 1999, *ApJ*, in press
- Mighell, K.J., Rich, R.M., Shara, M., & Fall, S.M. 1996, *AJ*, 111, 2314
- Mighell, K.J., Sarajedini, A., French, R.S. 1998, *AJ*, 116, 2395
- Mould, J.R., Da Costa, G.S., & Crawford, M.D. 1984, *ApJ*, 282, 125
- Mould, J.R., Jensen, J.B., & Da Costa, G.S. 1992, *ApJS*, 82, 489
- Olsen, K.A.G., Hodge, P.W., Mateo, M., Olszewski, E.W., Schommer, R.A., Suntzeff, N.B., & Walker, A.R. 1998, *MNRAS* 300, 665
- Olszewski, E.W., Suntzeff, N.B. & Mateo, M.M. 1996, *ARAA*, 34, 511 (OSM96)
- Olszewski, E.W., Schommer, R.A., Aaronson, M.A. 1987, *AJ*, 93, 565

- Udalski, A., Szymanski, M., Kubiak, M., Pietrzynski, G., Wozniak, P., & Zebrun, K. 1998, *Acta Astron.* 48, 1.
- van den Bergh, S. 1981, *A&AS*, 46, 79
- van den Bergh, S. 1991, *ApJ* 369, 1 (vdB91)
- Rich, R.M., Shara, M.M., Fall, S.M., & Zurek, D.M. 1999 in preparation
- Shara, M.M., Fall, S.M., Rich, R.M., & Zurek, D. 1998, *ApJ*, 508, 570
- ed. G. H. Jacoby, *PASP Conf. Ser.* 8, 289
- Stetson, P.B. 1994a, *PASP* 106, 250
- Stetson, P.B. 1994b, in *Proceedings of HST Calibration Workshop, Calibrating the Hubble Space Telescope*, ed. J.C. Blade and S.J. Osmer (Baltimore:STScI), 89
- Stryker, L.L., Da Costa, G.S., & Mould, J.R. 1985, *ApJ*, 298, 544
- Sweigart, A.V., Greggio, L., & Renzini, A. 1990, *ApJ*, 364, 527
- Walker, A.R. 1992, *ApJ*, 390, 81
- Westerlund, B.E. 1997, in *The Magellanic Clouds*, Cambridge University Press, Cambridge

Fig. 1.— The empirical ridgeline of NGC 411 is superposed on data from the HST Planetary Camera for NGC 152, 419, and 411 in the SMC, the “NGC 411” 2 Gyr burst group). The lower right panel shows the ridgelines (aligned using the red clump) and the Bertelli et al. (1994) isochrones. The best fit is for an age of 2 Gyr.

Fig. 2.— The empirical ridgeline of Kron 3 is superimposed on data from the HST Planetary Camera for NGC 339, 361, 416, and Kron 3 in the SMC (the “Kron 3” 8 Gyr burst group). Notice that the four clusters have nearly identical principle sequences: turnoff, red giant branch, and horizontal branch. Within the quality of the data, there is no visible dispersion in age, metallicity, or any other parameter between these clusters

Fig. 3.— (*Left Panel:*) The principle sequences of the 4 clusters in the 8 Gyr group are aligned to match each other as closely as possible. Also plotted on this figure are the loci of Lindsay 1 and NGC 121, which are illustrated because they are older. Because the physical depth of the SMC is large, we tie the CMD loci at the red clump to produce this comparison. The dispersion in main sequence turnoff loci of the 8 Gyr group clusters is consistent with being purely due to observational uncertainty. (*Right Panel:*) The Bertelli et al. (1994) isochrones are fit to the Kron 3 ridgeline; the isochrones and the ridgeline are aligned using the red clump. The best fit isochrone corresponds to 8 Gyr.

Fig. 4.— (*Upper Panel:*) The age distribution of old SMC clusters from Westerlund (1997) illustrates the continuous age distribution inferred from early studies. (*Middle Panel:*) The age distribution derived from our complete sample of clusters with $M_V < -6$; notice the two very clear bursts. (*Lower Panel:*) Full sample of > 1 Gyr old SMC clusters with color-magnitude diagram; this sample includes clusters as faint as $M_V = -5$.

TABLE 1
JOURNAL OF OBSERVATIONS

Cluster	Date (dd/mm/yy)	Filter	colheadExposure Time (Seconds)
NGC 152	26/09/94	F450W	300.0
	26/09/94	F555W	160.0
NGC 339	07/04/94	F450W	400.0
	07/04/94	F555W	200.0
NGC 361	03/04/94	F450W	300.0
	03/04/94	F555W	160.0
NGC 411	25/05/94	F450W	400.0
	25/05/94	F555W	200.0
NGC 416	06/02/94	F450W	400.0
	06/02/94	F555W	200.0
NGC 419	08/04/94	F450W	400.0
	08/04/94	F555W	200.0
KRON 3	27/05/94	F450W	600.0
	27/05/94	F555W	300.0

TABLE 2
APERATURE CORRECTIONS

Cluster	F555W (mag)	F450W (mag)
NGC 152	0.1849	0.2213
NGC 339	0.1704	0.1775
NGC 361	0.1729	0.1974
NGC 411	0.2014	0.2040
NGC 416	0.2033	0.2242
NGC 419	0.1927	0.1833
KRON 3	0.1802	0.2021

TABLE 3
PRE/POST COOL DOWN CORRECTIONS

Cluster	F555W (mag)	F450W (mag)
NGC 152	0.000	0.000
NGC 339	-0.062	-0.078
NGC 361	-0.062	-0.077
NGC 411	0.000	0.000
NGC 416	-0.062	-0.080
NGC 419	-0.062	-0.078
KRON 3	0.000	0.000

TABLE 4
CONTAMINATION CORRECTIONS

Cluster	F555W (mag)	F450W (mag)
NGC 152	-0.001	-0.001
NGC 339	-0.007	-0.004
NGC 361	-0.005	-0.003
NGC 411	0.000	0.000
NGC 416	-0.007	-0.004
NGC 419	-0.014	-0.008
KRON 3	-0.002	-0.001

TABLE 5
CLUSTER OFFSETS FOR FIT

Cluster	δV (mag)	$\delta B-V$ (mag)
NGC 121	-0.22	-0.11
NGC 152	0.00	0.00
NGC 339	+0.13	-0.09
NGC 361	+0.02	-0.06
NGC 411	+0.20	-0.06
NGC 416	-0.28	-0.10
NGC 419	+0.16	-0.02
KRON 3	0.00	0.00
LINDSAY 1	+0.11	-0.16

TABLE 6
KRON 3 RIDGELINE

B-V	V
0.398	23.873
0.377	23.702
0.357	23.470
0.335	23.232
0.307	22.945
0.293	22.713
0.288	22.530
0.281	22.353
0.281	22.191
0.282	22.061
0.293	21.983
0.318	21.918
0.356	21.868
0.398	21.843
0.440	21.818
0.486	21.818
0.516	21.823
0.533	21.806
0.552	21.781
0.570	21.735
0.580	21.671
0.592	21.574
0.606	21.409
0.618	21.160
0.625	20.953
0.640	20.488
0.664	20.214
0.687	19.965
0.720	19.704
0.748	19.443
0.780	19.269
0.808	19.045
0.874	18.647
0.976	18.100
1.112	17.541
1.341	16.969
1.485	16.857
1.653	16.819

TABLE 7
NGC 419 RIDGELINE

B-V	V
0.486	23.372
0.444	23.111
0.365	22.738
0.318	22.353
0.285	22.092
0.271	21.967
0.239	21.793
0.220	21.582
0.206	21.420
0.187	21.246
0.183	21.097
0.183	20.997
0.173	20.898
0.173	20.774
0.173	20.660
0.169	20.528
0.184	20.411
0.229	20.312
0.293	20.254
0.345	20.254
0.416	20.295
0.453	20.362
0.506	20.411
0.565	20.486
0.606	20.519
0.666	20.561
0.718	20.519
0.734	20.363
0.748	20.251
0.757	20.139
0.775	19.964
0.797	19.723
0.816	19.574
0.836	19.369
0.869	19.095
0.898	18.903
0.930	18.697
0.981	18.336
1.004	18.138
1.032	17.988
1.088	17.653
1.144	17.404
1.201	17.205
1.243	17.056
1.275	16.956
1.294	16.894

TABLE 8
KRON 3 HB RIDGELINE

B-V	V
0.664	19.493
0.640	19.493
0.612	19.493
0.575	19.480
0.542	19.493
0.505	19.480
0.472	19.480

TABLE 9
NGC 419 HB RIDGELINE

B-V	V
0.743	19.443
0.724	19.456
0.706	19.443
0.682	19.456
0.659	19.468
0.626	19.456
0.594	19.468
0.557	19.468
0.519	19.468

TABLE 10
CLUSTER AGE DETERMINATIONS FROM ISOCHRONE FITS

Cluster	Method	[Fe/H]=-1.71 t (Gyr)	[Fe/H]=-1.31 t (Gyr)	[Fe/H]=-0.71 t (Gyr)
NGC 152	SMC mod only	1.8 - 2.5	1.6 - 2.2	1.3 - 2.0
	mod + shift	1.8 - 2.5	2.0 - 2.5	1.3 - 1.8
	forced HB fit	1.0 - 1.4	1.6 - 2.2	1.3 - 1.8
NGC 411	SMC mod only	1.3 - 2.0	1.4 - 2.2	1.0 - 1.6
	mod + shift	1.3 - 2.0	1.3 - 2.0	1.0 - 1.6
	forced HB fit	0.8 - 1.3	1.3 - 2.0	1.3 - 1.8
NGC 419	SMC mod only	1.3 - 2.2	1.4 - 2.2	1.0 - 1.8
	mod + shift	1.6 - 2.2	1.8 - 2.2	1.0 - 1.6
	forced HB fit	0.8 - 1.3	1.3 - 2.0	1.3 - 1.8
Kron 3	SMC mod only	7.1 - 8.9	5.6 - 7.9	3.5 - 5.6
	mod + shift	7.1 - 8.9	5.6 - 7.1	4.5 - 5.6
	forced HB fit	7.1 - 8.9	7.1 - 8.9	6.3 - 7.1
NGC 339	SMC mod only	6.3 - 10.0	5.0 - 7.9	3.5 - 5.6
	mod + shift	5.0 - 6.3	4.0 - 5.0	2.8 - 3.5
	forced HB fit	7.1 - 8.9	7.1 - 8.9	6.3 - 7.1
NGC 361	SMC mod only	7.1 - 10.0	6.3 - 8.9	4.0 - 6.3
	mod + shift	7.1 - 8.9	5.0 - 6.3	3.5 - 4.5
	forced HB fit	7.9 - 10.0	7.9 - 8.9	7.1 - 8.9
NGC 416	SMC mod only	8.9 - 11.2	7.1 - 11.2	4.0 - 7.1
	mod + shift	7.1 - 8.9	5.6 - 7.1	4.0 - 5.0
	forced HB fit	7.9 - 8.9	7.1 - 8.9	5.6 - 7.1

TABLE 11
CLUSTER AGE DETERMINATIONS FROM ISOCHRONE FITS

Cluster	Method	[Fe/H]=-1.71 t (Gyr)	[Fe/H]=-1.31 t (Gyr)	[Fe/H]=-0.71 t (Gyr)
NGC 411	SMC mod only	1.58 - 2.11	1.78 - 2.00	1.26 - 1.58
	mod + shift	1.58 - 2.11	1.58 - 2.11	1.26 - 1.50
	forced HB fit	1.00 - 1.19	1.58 - 2.11	1.26 - 1.50
Kron 3	SMC mod only	7.94 - 10.0	6.31 - 8.91	4.47 - 6.31
	mod + shift	5.62 - 7.94	4.47 - 7.24	3.16 - 5.62
	forced HB fit	7.94 - 8.91	7.94 - 8.41	6.31 - 7.94